PROCEEDINGS A

rspa.royalsocietypublishing.org

Research

Cite this article: Loudon R. 2016 One-dimensional hydrogen atom. *Proc. R. Soc. A* **472**: 20150534.
http://dx.doi.org/10.1098/rspa.2015.0534

Received: 2 August 2015
Accepted: 1 December 2015

Subject Areas:
optics

Keywords:
Coulomb potential, singular and cut-off forms, high magnetic fields, semiconductor quantum wires, carbon nanotubes, polymer chains

Author for correspondence:
Rodney Loudon
e-mail: loudr@essex.ac.uk

One-dimensional hydrogen atom

Rodney Loudon

School of Computer Science and Electronic Engineering, University of Essex, Colchester CO4 3SQ, UK

The theory of the one-dimensional (1D) hydrogen atom was initiated by a 1952 paper but, after more than 60 years, it remains a topic of debate and controversy. The aim here is a critique of the current status of the theory and its relation to relevant experiments. A 1959 solution of the Schrödinger equation by the use of a cut-off at $x = a$ to remove the singularity at the origin in the $1/|x|$ form of the potential is clarified and a mistaken approximation is identified. The singular atom is not found in the real world but the theory with cut-off has been applied successfully to a range of four practical three-dimensional systems confined towards one dimension, particularly their observed large increases in ground state binding energy. The true 1D atom is in principle restored when the short distance a tends to zero but it is sometimes claimed that the solutions obtained by the limiting procedure differ from those obtained by solution of the basic Schrödinger equation without any cut-off in the potential. The treatment of the singularity by a limiting procedure for applications to practical systems is endorsed.

1. Introduction

The one-dimensional (1D) hydrogen (H) atom has a Coulomb potential equivalent to a 1D version of its usual three-dimensional (3D) form, with Schrödinger equation

$$-\frac{\hbar^2}{2m}\frac{\mathrm{d}^2\psi}{\mathrm{d}x^2} - \frac{e^2}{4\pi\varepsilon_0|x|}\psi = E\psi, \tag{1.1}$$

in SI units. The $1/|x|$ singularity in one dimension is much more serious than the $1/r$ singularity in three dimensions, because the effects of the latter are largely neutralized by the 3D spatial volume proportional to r^2 centred on $r = 0$. As a purely mathematical problem, it follows from the general theory of singular differential equations, as in Whittaker & Watson [1], that equation (1.1) does not have a complete set of solutions. There is a complete

THE ROYAL SOCIETY PUBLISHING

set of well-behaved odd-parity solutions, as the potential term on the left of equation (1.1) is finite for such wave functions, but well-behaved even-parity solutions are absent. The lack of these solutions is not acceptable for a problem in quantum mechanics. With only odd-parity functions it is, for example, impossible to form wave-packets with the particle localized in the $x < 0$ or $x > 0$ half spaces. These considerations rule out the validity of the original treatment of the 1D H atom by Flügge & Marschall [2], who found only the odd-parity solutions.

In 1957, Willis Lamb suggested that the very strong singularity in one dimension could be tamed by the insertion of a cut-off at a small distance a from the origin, so that the potential at $x = 0$ has a large but finite negative value. A theory for such *cut-off* potentials [3] considered two forms. They remove the singularity and both have similar effects on the energy levels. One of them, illustrated in fig. 2 of [3], is

$$V(x) = \frac{-e^2}{4\pi\varepsilon_0(a + |x|)}. \tag{1.2}$$

The solutions of the Schrödinger equation for this form are summarized in §2. It is used here as it provides a reasonable approximation for four applications of the theory considered in §3.

The many publications that criticize the theory based on a cut-off potential are discussed in §4. It is concluded that attempts to solve the singular equation (1.1) are inhibited by the basic mathematical theory mentioned above. Such solutions are in any case irrelevant for the applications to physical systems outlined in §3. Our overall conclusions are presented in §5.

2. Forms of solution

The properties of the 1D atom are conveniently expressed in terms of the Bohr radius and Rydberg energy of the 3D H atom, respectively

$$a_0 = \frac{4\pi\varepsilon_0\hbar^2}{me^2} = 5.3 \times 10^{-11}\ \mathrm{m} \tag{2.1}$$

and

$$R = \frac{\hbar^2}{2ma_0^2} = \frac{m}{2\hbar^2}\left(\frac{e^2}{4\pi\varepsilon_0}\right)^2 = 2.18 \times 10^{-18}\ \mathrm{J}. \tag{2.2}$$

An effective quantum number α for the 1D H atom is defined by

$$E = -\frac{R}{\alpha^2}, \tag{2.3}$$

and a modified position variable w by

$$\begin{aligned} w &= \frac{2(a + x)}{a_0\alpha} \quad \text{for} \quad x > 0 \\ &= \frac{-2(a - x)}{a_0\alpha} \quad \text{for} \quad x < 0. \end{aligned} \tag{2.4}$$

Replacement of the singular potential in equation (1.1) by the cut-off form in equation (1.2) now leads to the Schrödinger equation

$$\frac{\mathrm{d}^2\psi}{\mathrm{d}w^2} + \frac{\alpha\,\psi}{|w|} - \frac{\psi}{4} = 0, \tag{2.5}$$

which is a simple form of the *confluent hypergeometric equation*, with well-known solutions [4]. The allowed values of α, and thus the wave functions and energy levels, are determined by connection of the solutions of equation (2.5) for positive and negative x or w. The solutions of equation (1.1) for the 1D H atom with the singular potential are then obtained by taking the limit $a \to 0$.

The lengthy calculations for solution of the Schrödinger equation (2.5), fully described in [3], are not repeated here. The main results are instead clarified and summarized, with a discussion

of their features. The bound-state energies of the 1D H atom with cut-off potential are given by a Balmer-like formula. It is convenient to define a positive normalized cut-off distance β by

$$\beta = \frac{a}{a_0}, \quad \text{so that } V(x) = \frac{-e^2}{4\pi\varepsilon_0(\beta a_0 + |x|)}. \tag{2.6}$$

Normalized binding energies $e_{n\pm}$ are defined by

$$e_{n\pm} \equiv -\frac{E_{n\pm}}{R} = \frac{1}{\alpha_{n\pm}^2} \quad \text{with } n = 0, 1, 2, \ldots, \tag{2.7}$$

where the $n = 0$ level is additional to the 3D Balmer formula. There is no odd-parity state for $n = 0$ but all of the excited states occur with both even and odd parities, denoted by the $+$ or $-$ subscript, respectively. The energy of the even-parity ground state is determined by the eigenvalue condition in eqn (3.28) of [3], re-expressed as

$$\beta = \frac{\exp\left(-\frac{1}{2}\sqrt{e_0}\right)}{2\sqrt{e_0}}. \tag{2.8}$$

The binding energies of the excited states are determined by eqns (3.25) and (3.26) of [3] as

$$\alpha_{n-} \approx n + 2\beta \tag{2.9}$$

and

$$\beta = \tfrac{1}{2}\alpha_{n+} \exp\left(\frac{-1}{\alpha_{n+} - n}\right). \tag{2.10}$$

These excited-state energies are all smaller than their respective Balmer values.

The odd-parity expression (2.9) is simple but the even-parity expressions (2.8) and (2.10) awkwardly express cut-off distances β for given binding energies. The ground state is of most importance for many of the applications covered in §3 and relation (2.8) can be inverted as

$$e_0 = 4W^2\left(\frac{1}{4\beta}\right), \tag{2.11}$$

where W is the Lambert function [5]. This relation is equivalent to equation (2.8) and their common continuous curve in figure 1 shows that large binding energies e_0 occur even for the relatively large cut-off distances represented towards the right-hand end of the β-axis.

It is claimed in [3] that equations (2.8) and (2.10), already somewhat approximate, can be further approximated as

$$e_0' \approx 4\ln^2(2\beta) \quad \text{and} \quad \alpha_{n+}' \approx \frac{n-1}{\ln(2\beta/n)}. \tag{2.12}$$

These approximations are inaccurate for the values of β that can be achieved for practical systems. The ground state approximation is particularly poor, and the broken curve in figure 1 shows e_0' as a function of β, consistently much larger than e_0 obtained from equation (2.8). The asymptotics of the Lambert W function lead to a better ground state approximation than in equation (2.12). The discrepancies are smaller for the excited states but the approximations in equation (2.12) are generally poor.

For a typical value of the normalized cut-off distance, the binding energies of the three lowest levels are obtained from equations (2.8)–(2.10) as

$$e_0 \approx 22, \quad e_{1-} \approx 0.96 \quad \text{and} \quad e_{1+} \approx 0.64 \quad \text{for } \beta = 10^{-2}. \tag{2.13}$$

The large ground state binding energy agrees with figure 1 and the energies of the $n = 1$ states are very significantly split. The increase in the cut-off potential relative to the singular potential close to $x = 0$ has a larger effect on the even-parity states than on the odd-parity states. The excited-state probability densities extend over distances of the order of the Bohr radius a_0 on both sides of $x = 0$.

The cut-off potential tends to the singular potential in equation (1.1) for $\beta \to 0$. The binding energies are then given by equation (2.7) with $\alpha_{n\pm}$ set equal to n. The pairs of excited odd- and

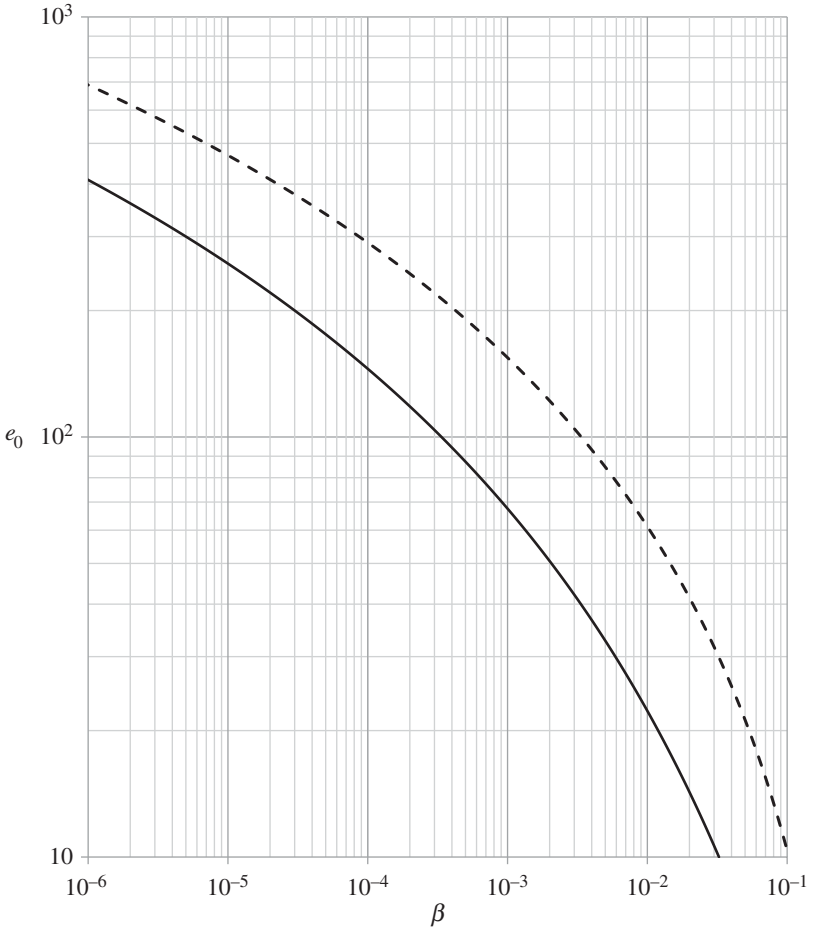

Figure 1. Solid curve: normalized ground state energy e_0 from equation (2.8) or equation (2.11) as a function of normalized cut-off distance β. Dashed curve: more approximate form e_0' from equation (2.12).

even-parity states tend towards twofold degeneracy, with the same energy levels as those of the 3D H atom. The normalized wave functions are [3]

$$\psi(o,e) = \sqrt{\frac{2}{a_0^3 n^5 (n!)^2}} \exp\left(\frac{-|x|}{na_0}\right) L_n^1\left(\frac{2|x|}{na_0}\right)(x,|x|) \quad \text{with } n = 1,2,\ldots, \tag{2.14}$$

where L_n^1 is an associated Laguerre polynomial and the even-parity wave function is obtained from the odd by simple replacement of x by $|x|$ in the final factor. The $n=1$ wave functions are plotted in fig. 5 of [3]. The binding energy of the non-degenerate even-parity $n=0$ ground state tends to infinity as $\alpha_0 \to 0$. There is often a particular interest in this state, with its wayward increase in binding energy well beyond the Rydberg value R for the 3D H atom, as in figure 1 and the numerical example in equation (2.13). The ground state wave function in the limit of the singular potential is

$$\psi_0 = \operatorname*{Lt}_{\alpha\to 0} (\alpha\, a_0)^{-1/2} \exp\left(\frac{-|x|}{\alpha\, a_0}\right), \quad \text{so that } |\psi_0|^2 = \delta(x), \tag{2.15}$$

with the electron localized at the origin. This limit is not even remotely approached for the practical systems so far studied, whose β-values lie close to the right-hand end of the horizontal axis in figure 1.

3. Applications of the theory

(a) Method of approximation

A common approximation for the main examples of 3D systems that can show a tendency to 1D behaviour is based on an assumption that the Coulomb energy of the 3D atom is overwhelmed by the energy of forces in the yz-plane that confine the charges towards one dimension. These forces lead to a transverse extension a of the wave function that is much smaller than the Bohr radius a_0, with a correspondingly small value for the normalized cut-off distance β. The transverse part $\psi(y,z)$ of the complete wave function is assumed to retain its form in the absence of the Coulomb interaction. It satisfies the normalization condition

$$1=\int_{-\infty}^{\infty}\mathrm{d}y\int_{-\infty}^{\infty}\mathrm{d}z\,|\psi(y,z)|^2=\int_0^{\infty}\mathrm{d}\rho\int_0^{2\pi}\mathrm{d}\phi\rho\,|\psi(\rho,\phi)|^2=2\pi\int_0^{\infty}\mathrm{d}\rho\rho\,|\psi(\rho)|^2\,, \tag{3.1}$$

with the y,z Cartesian coordinates changed to two-dimensional (2D) polar coordinates ρ, ϕ and a constant phase then assumed for the azimuthal dependence. The 1D potential for the x-motion is now approximated as a transverse average over the Coulomb potential

$$V(x)=-\frac{e^2}{2\varepsilon_0}\int_0^{\infty}\mathrm{d}\rho\frac{\rho}{\sqrt{\rho^2+x^2}}\,|\psi(\rho)|^2\,. \tag{3.2}$$

This integral is evaluated numerically for some of the applications that follow but two of its main features are very simply obtained. Thus, with the peak of the charge density $|\psi(\rho)|^2$ close to $\rho\approx a$, it follows from equations (3.1) and (3.2) that

$$V(|x|\gg a)\approx\frac{-e^2}{4\pi\varepsilon_0|x|}\quad\text{and}\quad V(0)\approx\frac{e^2}{4\pi\varepsilon_0 a}, \tag{3.3}$$

in support of the cut-off form of the 1D potential in equation (1.2). More accurate numerical calculations in the examples outlined below reinforce the use of a cut-off form for the 1D Coulomb potential, but the main emphasis in practice is often a striking increase in the ground state binding energy.

(b) Hydrogen atoms in high magnetic fields

The application of a large x-directed magnetic field $\boldsymbol{B}$ to a 3D H atom confines the electron towards a line parallel to $\boldsymbol{B}$ passing through the proton. The conversion to a 1D H atom is in principle complete for infinite B. The strength of the magnetic field is conveniently expressed in terms of the typical orbital radius of a charge e in the field, given by Landau & Lifshitz [6] as

$$a_B=\sqrt{\frac{\hbar}{eB}}. \tag{3.4}$$

The normalized cut-off distance in this example is thus defined by

$$\beta_B\equiv\frac{a_B}{a_0}=\sqrt{\frac{B_o}{B}}\quad\text{with}\quad B_0=2.3\times10^5\,\mathrm{T}\,(2.3\times10^9\,\mathrm{G}). \tag{3.5}$$

The spherical charge-density distribution of the zero-field 3D H atom changes to a cigar shape for magnetic fields B much larger than B_0, when $\beta_B\ll1$. The motion parallel to the x-axis, with a radius of order a_0, is controlled by the Coulomb potential of the nucleus but the motion in the yz-plane, with a radius of order a_B, is controlled by the magnetic field. The ground state is an exception, with its tendency towards localization at the origin, as in equation (2.15).

This first example of the 3D H atom confined towards one dimension was treated in [7,8] by use of the approximation outlined in §3a, with the Coulomb energies of order R treated as much

smaller than the energies associated with the applied magnetic field, of order [6]

$$E_B = \frac{e\hbar B}{2m}. \tag{3.6}$$

Here $R \ll E_B$ is equivalent to $B \gg B_0$, and the resulting potential is well approximated by that in equation (1.2). The method is outlined by Landau & Lifshitz [6] (§112, problem 3), confirming results derived for this case in [3,7]. The complete specification of states in magnetic fields needs an additional quantum number for the x component of angular momentum.

The highest available magnetic fields B are of order 20 T and the high-field region for hydrogen cannot be studied in the laboratory. However, the magnetic fields encountered in astrophysics often exceed B_0 from equation (3.5); for example, in the atmospheres of white dwarf and neutron stars, where magnetic fields of order 10^7–10^9 T occur, with β_B of order 10^{-1}–10^{-2}. The smallest value in this range approaches the condition for validity of the 1D H atom approximation. The most comprehensive account of the effects of high magnetic fields on atoms is given by Ruder *et al.* [9], who identify three regimes of field strength:

(i) *Weak field*, where the Coulomb potential predominates and the magnetic field provides a small perturbation. This is the regime of the linear and quadratic Zeeman effects.
(ii) *Intense field*, where the magnetic field predominates and the Coulomb potential provides a small perturbation. This is the regime of the 1D H atom with a cut-off potential.
(iii) *Intermediate or strong field*, with comparable strengths of Coulomb potential and magnetic field.

They provide extensive high-accuracy numerical calculations that apply all the way from the ordinary 3D H atom in zero magnetic field to the very high fields present in appropriate stars. The calculated H atom binding energies as functions of the applied magnetic field B are shown in fig. 4.1 of [9]. Many of the 3D excited-state energies move from a weak-field Balmer level towards a 1D level with smaller principal quantum number n as the field increases from small to large values. The lowest group of levels, destined for the 1D ground state, shows the usual large increase in binding energy at the highest fields B.

The variations with B of the energies of the lowest levels with zero angular momentum x-component for the intense-field regime are shown in figure 2, adapted from fig. 1 of [10] with appropriate changes in notation. These levels are of most relevance for comparisons with previous work and later examples in the present section. The range of B fields is converted by equation (3.5) to the range of normalized cut-off distances

$$2.24 \times 10^{-1} \geq \beta_B \geq 7.07 \times 10^{-3}. \tag{3.7}$$

The tendencies of the pairs of excited states towards the Rydberg energies are clearly visible and their binding energies at the highest fields are in very good agreement with the predictions of 1D H atom theory. The 1D ground state binding energy from equations (2.8) or (2.11) is a little smaller than that provided by the more accurate numerical calculations [9,10], with respective e_0 values of 27 and 34 at the highest magnetic field in figure 2. Comparisons of the theory for these high magnetic fields with actual measured values are scarce.

There are useful reviews of the field up to 1977 by Garstang [11], up to 1989 by Friedrich & Wintgen [12] and very recently by Potekhin [13].

Another high magnetic-field application is to the exciton in a semiconductor, described by Orton [14]. This H-atom-like object is formed by excitation of an electron from the highest valence band to the lowest conduction band, leaving a positively charged 'hole' behind. In the *effective-mass approximation*, a theory similar to that of the H atom applies, with the Coulomb attraction reduced by the relative permittivity ε of the semiconductor and the free-electron mass m replaced by the reduced effective mass μ of the exciton, defined by

$$\mu = \frac{m_\mathrm{e} m_\mathrm{h}}{m_\mathrm{e} + m_\mathrm{h}}, \tag{3.8}$$

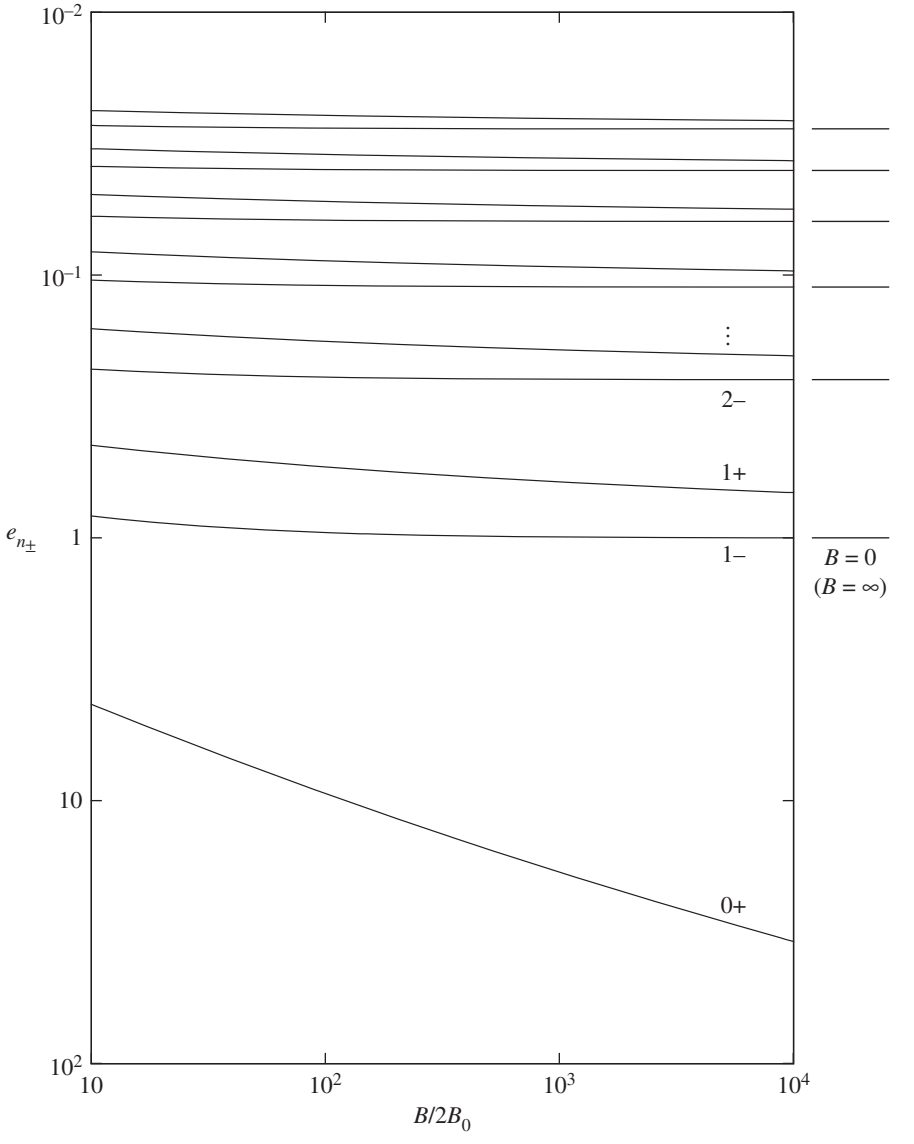

Figure 2. Calculated energies of the 13 lowest levels of the H atom with zero angular momentum x-component in high magnetic fields B. (Adapted from Wunner & Ruder [10].)

where m_e and m_h are the electron and hole effective masses. Then equations (2.1) and (2.2) convert to

$$\left.\begin{aligned} a_{0m} &= \frac{4\pi\varepsilon_0\varepsilon\hbar^2}{\mu e^2} = 1.24\times10^{-8}\,\mathrm{m} \\ \text{and}\qquad R_m &= \frac{\mu}{2\hbar^2}\left(\frac{e^2}{4\pi\varepsilon_0\varepsilon}\right)^2 = 7.11\times10^{-22}\,\mathrm{J}, \end{aligned}\right\} \tag{3.9}$$

where the m subscripts denote these modified expressions for material media. The numerical values here refer to GaAs, where $\varepsilon = 13.1$ and $\mu = 0.056m$, with changes in the theory that can increase the Bohr radius and decrease the Rydberg energy by substantial amounts. Thus, the value of the field B_{0m} needed for equality of the magnetic and Bohr radii in equation (3.5) is reduced to about 4 T for GaAs and 0.5 T for Ge, within the range of laboratory fields. Unfortunately,

these semiconductors have complicated energy-band structures, with degenerate fluted valence bands and ellipsoidal conduction bands, sometimes at different wavevectors in the Brillouin zone [14]. The simple form of effective-mass approximation does not then apply, impeding clear-cut comparisons of measured absorption spectra and theory [7,8].

(c) Semiconductor quantum wires

The subjection of a 3D H atom to a high magnetic field reconfigures it towards the condition of a 1D H atom but this can be achieved in other ways. Thus, a material fibre, with cross-sectional dimensions much smaller than the appropriate Bohr radius, accomplishes the same end, apparently more straightforwardly. Semiconductor quantum wires have various cross-sections, for example the common T fibre, but we consider here only cylindrical wires with radii a_{sqw} ideally much smaller than a_0. The radius plays the role of a potential cut-off distance, with normalized value

$$\beta_{\mathrm{sqw}} = \frac{\gamma a_{\mathrm{sqw}}}{a_{0\mathrm{m}}}, \tag{3.10}$$

where γ, of order unity, is determined by the cylinder boundary conditions. The 1D H atom theory again approaches a reasonable approximation for the energy levels of an exciton or hydrogenic impurity in the wire when β_{sqw} is of order 10^{-2} or smaller. In contrast to the awkward inverse square-root dependence of the normalized cut-off distance on the experimental variable B in equation (3.5), the linear dependence on the wire radius in equation (3.10) leads to the calculated variation of the ground state binding energy with β_{sqw} shown by the continuous curve in figure 1.

Banyai *et al.* [15], who originated the above form of the normalized cut-off distance, calculate the ground state binding energy of the exciton in GaAs cylinders embedded in $Ga_{1-x}Al_xAs$ as a function of the wire radius. They obtain numerical solutions by the separation of the x and yz motions outlined in §3a and find close agreement with results for the 1D cut-off potential when $\gamma = 0.3$, with a relation between normalized cut-off and ground state binding energy equivalent to equation (2.8). The exciton spectra measured by Katz *et al.* [16] in cylindrical CdSe quantum wires confirm that the energy-level structure is determined by the rod radius and not by its length. Shabaev & Efros [17] model the rods as ellipsoids of revolution, with an adiabatic separation of the motions parallel and perpendicular to the axis. Bartnik *et al.* [18] combine measurements on PbSe nanorods with a four-band effective-mass theory of the exciton spectra in its multi-valley structure. Their fig. 3 shows good agreement between the binding potential parallel to the x-axis calculated numerically and the form of 1D potential used in [7]. Their fig. 11 also shows good agreement between numerical and analytic calculations of the exciton probability densities for the ground and first excited states.

Slachmuylders *et al.* [19] calculate the lowest exciton levels in an infinitely long cylindrical nanowire again using an adiabatic decoupling of the motions parallel and perpendicular to the wire axis. Accurate numerical results for the resulting effective potential in the x-direction are fitted to simple analytical expressions. The calculations of ground and first excited-state energies in their fig. 6 cover the range of normalized cut-off distances

$$5 \times 10^{-4} \leq \beta_{\mathrm{sqw}} \leq 5. \tag{3.11}$$

The corresponding results obtained from equations (2.8) and (2.9) are also plotted in this figure, showing that the 1D H atom approximation is good for normalized cut-off distances less than about 10^{-2} for the ground state and about 10^{-1} for the first excited state.

The whole area of the optical properties of semiconductor structures of different dimensionalities is comprehensively reviewed by Haug & Koch [20]. Their §7.5 derives an explicit expression for the quasi-1D Coulomb potential by averaging the 3D Coulomb potential over radial yz envelope functions as in §3a and their fig. 7.4 shows its good fit to a cut-off potential as defined in equation (3.10) above with $\gamma = 0.3$. Their §10.3 provides a very useful summary of the energies and wave functions of the 3D, 2D and 1D excitons in succession, which greatly clarifies the contrasting behaviours for the different dimensionalities. Figs. 10.2–10.4 illustrate the

corresponding forms of the absorption spectra. The quasi-1D example in their fig. 10.4 shows a striking increase in ground state binding energy to $8R$ for a normalized cut-off distance of about 0.04, consistent with equations (2.8) and (2.11). The dominance of this state in the absorption spectrum is also emphasized, with its overwhelming share of the total oscillator strength. These trends of increasing binding energy and oscillator strength with decreasing dimensionality are useful in some practical applications [21].

Another aspect of reduced dimensionality is a calculated lifetime for the capture of electrons by attractive Coulomb centres in a cylindrical quantum wire [22] that is much shorter than for the same experiment in a 3D bulk semiconductor.

(d) Carbon nanotubes

This application of 1D H atom theory resembles the semiconductor quantum wire in its geometrical role of confining the transverse distribution of the exciton wave function to the system radius, again of the order of 10^{-9} m. Carbon nanotubes were discovered in the early 1990s and their properties are comprehensively reviewed by Charlier *et al.* [23]. They come in two basic varieties, multi-wall, with several concentric cylinders of increasing radii, and single-wall, with only one cylinder. The single-wall carbon nanotube (SWNT) consists of a 2D graphite layer, or graphene sheet, rolled up into a hollow cylinder of uniform radius. This system corresponds very closely to the approximation outlined in §3a and the properties of the 1D potential shown in equation (3.3) are valid.

The electronic properties of SWNTs depend upon the way in which the graphene sheet is rolled up to form a cylinder, denoted by a pair of integers (n, m), with the two possibilities [23]

$$\text{metallic for } n - m = 3l \quad \text{and} \quad \text{semiconducting for } n - m = 3l \pm 1, \tag{3.12}$$

where l is another integer. It follows statistically that one-third of all possible nanotubes are metallic and two-thirds are semiconducting. The tube radius is given by

$$a_{\text{cnt}} = 0.0391\sqrt{n^2 + nm + m^2}\ \text{nm}, \tag{3.13}$$

with a prefactor determined by the lattice constant of the graphene sheet.

The semiconducting SWNT, with the atomic-scale thickness of its cylindrical wall, is very different from the solid semiconducting cylinders considered in §3c and it has some advantages. Thus, Langbein (W Langbein 2013, personal communication) argues that the SWNT gives a closer approach to the 1D exciton than does the semiconducting quantum wire, on account of the former's better structural definition, with very little atomic disorder, the smaller dielectric screening associated with the tube structure and the low number of electrons in carbon. Also, the nanotubes can be fabricated with smaller radii, down to about 0.2 nm. The pioneering calculation by Ando [24] derived the exciton energy levels and absorption spectra for both semiconducting and metallic nanotubes. Pedersen [25] treats the exciton ground state by a variational method and obtains an improvement on equation (2.8) for its binding energy. Green-function calculations by Spataru *et al.* [26] for the (8,0) semiconducting nanotube find a significant increase in ground state exciton binding energy. Chang *et al.* [27] obtain a similar increase in a computation of the absorption spectrum of the (4,2) nanotube.

The optical properties of carbon nanotubes are intensively studied for the unprecedented tunability of their optical transition frequencies, with potential practical applications in opto-electronic devices and quantum information processing [28,29].

(e) Polymers

Our final application of 1D H atom theory is to calculations and measurements of impurity and exciton states in polymer-chain systems. The earliest studies, from 1982, report work on impurity states in doped *trans*-polyacetylene $(CH)_x$ chains. More substantial studies follow on the excitons in silicon polymer, polysilane, from 1991 to 1996 and in conjugated polymers from 1997 to the

present. These polymer systems here have quasi-1D chain-like structures quite different from the cylindrical symmetries of our previous examples. The relevant excitations are sometimes confined to a single chain, when the conversion from 3D to 1D geometry in §3a is no longer needed.

Early calculations by Bryant & Glick [30,31] treat the states associated with lightly doped $(CH)_x$, including the added feature that the dopant may lie on or off the chain axis at a distance a, respectively zero or of order 0.2 nm. They use the cut-off Coulomb potential

$$V(x) = \frac{-e^2}{4\pi\varepsilon_0\varepsilon\sqrt{a^2 + x^2}}, \tag{3.14}$$

different from the form in equation (1.2) but with the common values similar to equation (3.3). The variations of energy levels with a are obtained by numerical solution of a 1D effective-mass equation. The level structures resemble that of the 1D atom with a cut-off potential when $a > 0$ and that of the singular potential when $a = 0$. Despite the difference from equation (1.2), the theory outlined in §§2 and 3a provides a reasonable description of their numerical results. Thus, the Bohr radius is

$$a_0 = 3.63\,\text{nm} \tag{3.15}$$

for the parameter values of $(CH)_x$ and the normalized cut-off distance is

$$\beta_{t\text{-}p} = 5.5 \times 10^{-2} \quad \text{for } a = 0.2\,\text{nm}. \tag{3.16}$$

The numerical calculations predict an enhancement in ground state binding energy e_0 to $11R$, quite close to the value shown in figure 1.

The initial interpretations of measured polysilane spectra in terms of the 1D H atom were made by Moritomo *et al.* in 1991 [32] and subsequent work is dominated by Japanese contributions. Hasegawa *et al.* [33] report experimental and theoretical work on the 1D excitons in this silicon polymer, essentially a 1D semiconductor. They measure and calculate the one-photon linear and the two-photon third-order nonlinear optical spectra, obtaining the good agreement between experiment and theory shown in their fig. 2. Their very informative fig. 3, obtained by fitting theory to experiment, shows the variation of exciton envelope functions with x for the three lowest energy levels, in terms of a cut-off 1D Coulomb potential. These results confirm the dominance of the ground state in the optical absorption, with the usual striking increase in its binding energy. Its wave function clearly shows the linear exponential fall-off with $|x|$ apparent in ψ_0 given by equation (2.15) and the forms of the odd and even $n = 1$ excited-state wave functions resemble those in fig. 4 of [3]. Calculations by Hasegawa *et al.* [34] determine the variations of the binding energies of the first and second exciton levels as functions of the normalized cut-off distance for the potential in equation (1.2). They also discuss the natures of the physical origins of this potential.

The spectral properties of conjugated polymers are comprehensively described by Barford [35]. Liess *et al.* [36] made the first experimental and theoretical studies of the exciton states. Pedersen *et al.* [37] developed the theory for a single polymer chain confined in a 3D box, with an integration over the yz-plane, similar to that outlined in §3a. Their eqn (8) and fig. 2 show a 'soft effective potential' for the x motion similar to the cut-off potential in our equation (1.2). The exciton theory is further developed by Barford & Paiboonvorachat [38], who emphasize the role played by the centre-of-mass motion of the electron–hole pair, in addition to the relative motion considered previously. The resulting wave functions are products of the two contributions, with quantum numbers for each of the degrees of freedom. Their detailed forms in eqn (6.22) of [35] are consistent with equation (2.14) when the centre-of-mass dependence is ignored. Fig. F.2 of this reference, comparable with our figure 2, shows the binding energies of the four lowest levels, in units of the effective Rydberg, as functions of the lattice spacing, in units of the effective Bohr radius. The further details in [39] include the instructive figure 2, which shows the shapes and sizes of two low-lying exciton states as functions of the centre-of-mass and relative coordinates.

4. Criticisms of the basic theory

A large volume of work, amounting to about 100 publications, has criticized the results derived in [3] for the energy levels of the 1D H atom. The controversy mainly concerns the existence or the non-existence of the even-parity states and, if they do exist, their nature. There is thus a return to the original 1952 treatment of the 1D H atom [2]. Most of these papers aim to solve the Schrödinger equation (1.1) without any use of the limiting procedure, where a cut-off potential is converted continuously to the singular potential, as described in §2. There is no suggestion that the levels derived for the cut-off potential are incorrect, however small the length a, but it is implied that the genuine 1D atom differs discontinuously from its look-alike twin.

The theory of the 1D H atom in [3] was first criticized by Andrews in a very brief paper [40], claiming the non-existence of a ground state of infinite binding energy. Another early paper by Haines & Roberts [41] provides a much more comprehensive treatment, which unusually covers both the singular and the cut-off potentials. They show that the only discrete solutions of the wave equation (1.1) are those of odd parity, with energies identical to those of the 3D H atom. A set of even-parity states is also derived, with continuous ranges of energy that lie between the discrete levels and extend down to $-\infty$. The derivation in [41] for the cut-off potential finds the same results as [3] for both even and odd discrete states. The odd-parity solutions approach arbitrarily close to those for the singular potential as a tends to zero but the even-parity states change their natures from discrete to continuous. The continua of negative-energy even-parity states are in turn criticized by Andrews [42] for reasons including their non-orthogonality; the doubly degenerate even and odd excited states derived in [3] are restored but the non-existence of the $n = 0$ ground state is reaffirmed. All of the even-parity states are removed again by Gomes & Zimerman [43] but reinstated by Moss [44]. Debate on the solutions of the singular Schrödinger equation (1.1) persists, for example, in [45–47] and references therein.

The 1D H atom theory is reviewed by Barton [48], who is mainly concerned with the solution of its Klein–Gordon equation, but who also makes perceptive comments on the non-relativistic theory. He points out that the wave equation (1.1) with the singular potential is mathematically underdetermined, making it necessary either (i) to supplement it with matching conditions at the origin or (ii) to introduce a cut-off to soften the singularity there. Derivations that use method (i) are said to be apparently 'motivated purely by notions of mathematical simplicity', with consequent doubts as to their applicability to physical 1D systems. In the view of Barton, the mathematical options available for treatment of the singular potential cannot adequately elucidate the physics of the system. These remarks support the method outlined in §§1 and 2.

5. Conclusion

The 1D H atom is an abstract quantum-mechanical system apparently of only theoretical interest. Now 56 years after its treatment, no very close realizations have indeed been detected. There are, however, several examples of physical systems that show an approach to the ideal 1D atom, but always with a cut-off in the true Coulomb potential at short interaction distances. The ideal atom would be restored in the limit of zero cut-off distance but this cannot be achieved in practice. The relevant citations are mainly concerned with applications to 3D systems, where a variety of physical processes confine the motion in two of the dimensions. They employ a cut-off potential similar to that in equation (1.2) or other, often ingenious, methods of approximation to model the real experimental measurement. Several of the publications reviewed here present accurate calculations of the system energy levels for regimes intermediate between the 3D and the 1D H atoms; they have the satisfying feature that a 1D cut-off theory often emerges as correct in the appropriate limits of very strong magnetic field and very thin semiconductor fibre, carbon tube or polymer chain. A noteworthy feature of the quasi-1D atom is the increase in its binding energy well beyond the Rydberg value R for the 3D atom, a trend already evident for intermediate parameter values where the more accurate calculations are needed. The higher binding energies are useful in several practical applications.

The singular potential is retrieved in the limit of zero cut-off distance, with wave functions given by equations (2.14) and (2.15). The excited states become doubly degenerate, both even- and odd-parity wave functions tending to zero at $x = 0$; the singlet delta-function ground state acquires infinite binding energy. The nature of the solutions for the singular potential is a topic of continuing debate.

The procedure that led from the solution of a purely academic problem [3] to a subsequent discovery of practical applications is somewhat dismissed by Marcus & Davis [49]. They claim that it is better to fit a mathematical model to the real world than to design the model and then try to find something in the real world that fits. They quote John Maynard Smith, who described such models as 'theories looking for a question to answer'. While this opinion may be generally valid, the 1D H atom provides a worthy counter-example.

Data accessibility. The data as calculated are shown in figures 1 and 2.

Authors' contributions. I am the sole author and did all of the work myself.

Competing interests. I declare I have no competing interests.

Funding. I received no funding for this study.

Acknowledgements. I am particularly grateful to Willis Lamb, anonymous co-author of [3], who provided much help in calculating the properties of the 1D H atom. I thank Steve Barnett, Colin Baxter and Roger Elliott for their significant contributions, an anonymous referee for suggesting the ground state energy form shown in equation (2.11), Gabriel Barton, Alexander Efros, Wolfgang Langbein, John Orton, Günter Wunner and Nick Zakhleniuk for informative discussions, and Mary Loudon for improving the overall balance. Assistance with the acquisition of reprints and PDFs of many publications was kindly provided by Tsuneya Ando, William Barford (including his book [35] in PDF), Garnett Bryant, Joe Eberly, Tom Foxon, Harald Friedrich, Areg Ghazaryan, Richard Hall, Hartmut Haug, Colin Humphreys, John Jeffers, Cesar de Oliveira, Thomas Pedersen, Riccardo Rurali, Seiji Sakoda, Alvaro Salas-Brito, Marina Semina and Catalin Spataru. Stephan Koch very helpfully provided his publications and a paper copy of his book with Hartmut Haug [20]. I thank David Roberts, Christoph Schimezcek and particularly Stephen Smith for help with the figures.

References

1. Whittaker ET, Watson GN. 1927 *Modern analysis*. Cambridge, UK: Cambridge University Press.
2. Flügge S, Marschall H. 1952 *Rechenmethoden der Quantentheorie*. Berlin, Germany: Springer.
3. Loudon R. 1959 One-dimensional hydrogen atom. *Am. J. Phys.* **27**, 649–655. (doi:10.1119/1.1934950)
4. Slater LJ. 1960 *Confluent hypergeometric functions*. Cambridge, UK: Cambridge University Press.
5. Corless RM, Gonnet GH, Hare DEG, Jeffrey DJ, Knuth DE. 1996 On the Lambert W function. *Adv. Comp. Math.* **5**, 329–359. (doi:10.1007/BF02124750)
6. Landau LD, Lifshitz EM. 1977 *Quantum mechanics*. Oxford, UK: Pergamon Press.
7. Elliott RJ, Loudon R. 1960 Theory of the absorption edge in semiconductors in a high magnetic field. *J. Phys. Chem. Solids* **15**, 196–207. (doi:10.1016/0022-3697(60)90243-2)
8. Hasegawa H, Howard HE. 1961 Optical absorption spectrum of hydrogenic atoms in a strong magnetic field. *J. Phys. Chem. Solids* **21**, 179–198. (doi:10.1016/0022-3697(61)90097-X)
9. Ruder H, Wunner G, Herold H, Geyer F. 1994 *Atoms in strong magnetic fields*. Berlin, Germany: Springer.
10. Wunner G, Ruder H. 1981 Hydrogen atom in strong magnetic fields. *Astron. Astrophys.* **95**, 204–205.
11. Garstang RH. 1977 Atoms in high magnetic fields. *Rep. Prog. Phys.* **40**, 105–154. (doi:10.1088/0034-4885/40/2/001)
12. Friedrich H, Wintgen D. 1989 The hydrogen atom in a uniform magnetic field—an example of chaos. *Phys. Rep.* **183**, 37–79. (doi:10.1016/0370-1573(89)90121-X)
13. Potekhin AY. 2014 Atmospheres and radiating surfaces of neutron stars. *Phys. Uspekhi* **57**, 735–770. (doi:10.3367/UFNe.0184.201408a.0793)
14. Orton JW. 2004 *The story of semiconductors*. Oxford, UK: Oxford University Press.
15. Banyai L, Galbraith I, Ell C, Haug H. 1987 Excitons and biexcitons in semiconductor quantum wires. *Phys. Rev. B* **36**, 6099–6104. (doi:10.1103/PhysRevB.36.6099)

16. Katz D, Wizansky T, Millo O, Rothenberg E, Mokari T, Banin U. 2002 Size-dependent tunneling and optical spectroscopy of CdSe quantum rods. *Phys. Rev. Lett.* **89**, 086801. (doi:10.1103/PhysRevLett.89.086801)
17. Shabaev A, Efros AL. 2004 1D exciton spectroscopy of semiconductor nanorods. *Nano Lett.* **4**, 1821–1825. (doi:10.1021/nl049216f)
18. Bartnik AC, Efros AL, Koh WK, Murray CB, Wise FW. 2010 Electronic states and optical properties of PbSe nanorods and nanowires. *Phys. Rev. B* **82**, 195313. (doi:10.1103/PhysRevB.82.195313)
19. Slachmuylders AF, Partoens B, Magnus W, Peeters FM. 2006 Exciton states in cylindrical nanowires. *J. Phys. Condens. Matter* **18**, 3951–3966. (doi:10.1088/0953-8984/18/16/005)
20. Haug H, Koch SW. 2009 *Quantum theory of the optical and electronic properties of semiconductors.* Singapore: World Scientific.
21. Gibbs HM, Khitrova G, Koch SW. 2011 Exciton–polariton light–semiconductor coupling effects. *Nat. Photonics* **5**, 275–282. (doi:10.1038/nphoton.2011.15)
22. Zakhleniuk NA, Ridley BK. 1997 Cascade capture and hot photoelectrons in one-dimensional semiconductors. *Phys. Stat. Sol.* **204**, 287–289. (doi:10.1002/1521-3951(199711)204:1<287::AID-PSSB287>3.0.CO;2-B)
23. Charlier J-C, Blase X, Roche S. 2007 Electronic and transport properties of nanotubes. *Rev. Mod. Phys.* **79**, 677–732. (doi:10.1103/RevModPhys.79.677)
24. Ando T. 1997 Excitons in carbon nanotubes. *J. Phys. Soc. Jap.* **66**, 1066–1073. (doi:10.1143/JPSJ.66.1066)
25. Pedersen TG. 2003 Variational approach to excitons in carbon nanotubes. *Phys. Rev. B* **67**, 073401. (doi:10.1103/PhysRevB.67.073401)
26. Spataru CD, Ismail-Beigi S, Benedict LX, Louie SG. 2004 Excitonic effects and optical spectra of single-walled carbon nanotubes. *Phys. Rev. Lett.* **92**, 077402. (doi:10.1103/PhysRevLett.92.077402)
27. Chang E, Bussi G, Ruini A, Molinari E. 2004 Excitons in carbon nanotubes: an *ab initio* symmetry-based approach. *Phys. Rev. Lett.* **92**, 196401. (doi:10.1103/PhysRevLett.92.196401)
28. Franklin AD. 2013 The road to carbon nanotube transistors. *Nature* **498**, 443–444. (doi:10.1038/498443a)
29. Hofmann MS, Glückert JT, Noé J, Bourjau C, Dehmel R, Högele A. 2013 Bright, long-lived and coherent excitons in carbon nanotube quantum dots. *Nat. Nanotechnol.* **8**, 502–505. (doi:10.1038/nnano.2013.119)
30. Bryant GW, Glick AJ. 1982 Impurity states in doped *trans*-polyacetylene. *J. Phys. C: Solid State Phys.* **15**, L391–L396. (doi:10.1088/0022-3719/15/13/003)
31. Bryant GW, Glick AJ. 1982 The importance of impurity states in doped *trans*-polyacetylene. *Phys. Rev. B* **26**, 5855–5866. (doi:10.1103/PhysRevB.26.5855)
32. Moritomo Y, Tokura Y, Tachibana H, Kawabata Y, Miller RD. 1991 Excited states of one-dimensional excitons in polysilanes as investigated by two-photon spectroscopy. *Phys. Rev. B* **43**, 14 746–14 749. (doi:10.1103/PhysRevB.43.14746)
33. Hasegawa T, Iwasa Y, Sunamura H, Koda T, Tokura Y, Tachibana H, Matsumoto M, Abe S. 1992 Nonlinear optical spectroscopy on one-dimensional excitons in silicon polymer, polysilane. *Phys. Rev. Lett.* **69**, 668–671. (doi:10.1103/PhysRevLett.69.668)
34. Hasegawa T, Iwasa Y, Koda T, Kishida H, Tokura Y, Wada S, Tashiro H, Tachibana H, Matsumoto M. 1996 Nature of one-dimensional excitons in polysilanes. *Phys. Rev. B* **54**, 11 365–11 374. (doi:10.1103/PhysRevB.54.11365)
35. Barford W. 2013 *Electronic and optical properties of conjugated polymers*. Oxford, UK: Oxford University Press.
36. Liess M, Jeglinski S, Vardeny ZV, Ozaki M, Yoshino K, Ding Y, Barton T. 1997 Electro-absorption spectroscopy of luminescent and nonluminescent π-conjugated polymers. *Phys. Rev. B* **56**, 15 712–15 724. (doi:10.1103/PhysRevB.56.15712)
37. Pedersen TG, Johansen PM, Pedersen HC. 2000 Particle-in-a-box model of one-dimensional excitons in conjugated polymers. *Phys. Rev. B* **61**, 10 504–10 510. (doi:10.1103/PhysRevB.61.10504)
38. Barford W, Paiboonvorachat N. 2008 Excitons in conjugated polymers: wavefunctions, symmetries, and quantum numbers. *J. Chem. Phys.* **129**, 164716. (doi:10.1063/1.3001584)
39. Barford W. 2013 Excitons in conjugated polymers: a tale of two particles. *J. Phys. Chem. A* **117**, 2665–2671. (doi:10.1021/jp310110r)

40. Andrews M. 1966 Ground state of the one-dimensional hydrogen atom. *Am. J. Phys.* **34**, 1194–1195. (doi:10.1119/1.1972657)
41. Haines LK, Roberts DH. 1969 One-dimensional hydrogen atom. *Am. J. Phys.* **37**, 1145–1154. (doi:10.1119/1.1975232)
42. Andrews M. 1976 Singular potentials in one dimension. *Am. J. Phys.* **44**, 1064–1066. (doi:10.1119/1.10585)
43. Gomes JF, Zimerman AH. 1980 One-dimensional hydrogen atom. *Am. J. Phys.* **48**, 579–580. (doi:10.1119/1.12067)
44. Moss RE. 1987 The hydrogen atom in one dimension. *Am. J. Phys.* **55**, 397–401. (doi:10.1119/1.15144)
45. Gebremedhin DH, Weatherford CA. 2014 Calculations for the one-dimensional soft Coulomb problem and the hard Coulomb limit. *Phys. Rev. E* **89**, 053319. (doi:10.1103/PhysRevE.89.053319)
46. Carrillo-Bernal MA, Núnez-Yépez HN, Salas-Brito AL, Solis DA. 2015 Comment on 'Calculations for the one-dimensional soft Coulomb problem and the hard Coulomb limit'. *Phys. Rev. E* **91**, 027301. (doi:10.1103/PhysRevE.91.027301)
47. Pedersen TG. 2015 Analytic models of optical response in one-dimensional semiconductors. *Phys. Lett. A* **379**, 1785–1790. (doi:10.1016/j.physleta.2015.05.008)
48. Barton G. 2007 On the 1D Coulomb Klein–Gordon equation. *J. Phys. A: Math. Theor.* **40**, 1011–1031. (doi:10.1088/1751-8113/40/5/010)
49. Marcus G, Davis E. 2013 When it comes to science, maths must be part of the equation. *Financial Times*, 13/14 April 2013, p. 9, UK print-edition (p. 5, Asian and US print-editions).